

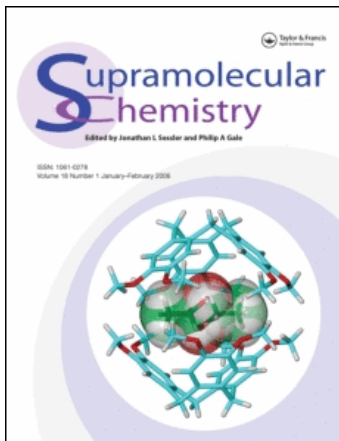
This article was downloaded by:

On: 29 January 2011

Access details: *Access Details: Free Access*

Publisher *Taylor & Francis*

Informa Ltd Registered in England and Wales Registered Number: 1072954 Registered office: Mortimer House, 37-41 Mortimer Street, London W1T 3JH, UK



Supramolecular Chemistry

Publication details, including instructions for authors and subscription information:

<http://www.informaworld.com/smpp/title~content=t713649759>

Alkali metal and ammonium cation-arene interactions with tetraphenylborate anion

Ruiqiong Li^a; Rudolph E. K. Winter^b; Joseph Kramer^b; George W. Gokel^{bc}

^a Department of Chemistry, Washington University, Saint Louis, MO, USA ^b Departments of Chemistry & Biochemistry and Biology, Center for Nanoscience, University of Missouri - Saint Louis, Saint Louis, MO, USA ^c Washington University School of Medicine, Saint Louis, MO, USA

First published on: 20 August 2009

To cite this Article Li, Ruiqiong , Winter, Rudolph E. K. , Kramer, Joseph and Gokel, George W.(2010) 'Alkali metal and ammonium cation-arene interactions with tetraphenylborate anion', *Supramolecular Chemistry*, 22: 2, 73 – 80, First published on: 20 August 2009 (iFirst)

To link to this Article: DOI: 10.1080/10610270903045318

URL: <http://dx.doi.org/10.1080/10610270903045318>

PLEASE SCROLL DOWN FOR ARTICLE

Full terms and conditions of use: <http://www.informaworld.com/terms-and-conditions-of-access.pdf>

This article may be used for research, teaching and private study purposes. Any substantial or systematic reproduction, re-distribution, re-selling, loan or sub-licensing, systematic supply or distribution in any form to anyone is expressly forbidden.

The publisher does not give any warranty express or implied or make any representation that the contents will be complete or accurate or up to date. The accuracy of any instructions, formulae and drug doses should be independently verified with primary sources. The publisher shall not be liable for any loss, actions, claims, proceedings, demand or costs or damages whatsoever or howsoever caused arising directly or indirectly in connection with or arising out of the use of this material.

Alkali metal and ammonium cation–arene interactions with tetraphenylborate anion

Ruiqiong Li^a, Rudolph E.K. Winter^b, Joseph Kramer^b and George W. Gokel^{bc*}

^aDepartment of Chemistry, Washington University, 1 Brookings Drive, Saint Louis, MO 63130, USA; ^bDepartments of Chemistry & Biochemistry and Biology, Center for Nanoscience, University of Missouri – Saint Louis, One University Boulevard, Saint Louis, MO 63121, USA; ^cWashington University School of Medicine, Saint Louis, MO, 63110, USA

(Received 15 March 2009; final version received 8 May 2009)

Sodium, potassium, rubidium, caesium, ammonium and tetramethylammonium tetraphenylborates were studied by both positive and negative ion electrospray mass spectrometry. An affinity order of $\text{Cs}^+ > \text{Rb}^+ > \text{K}^+ \sim \text{Na}^+$ was obtained. The results obtained were compared with both calculations and solid-state structures, where available. The previously reported high affinity of caesium for tetraphenylborate concluded from NMR experiments was confirmed for the gas phase. The affinity does not appear to result from steric effects and a cation– π interaction seems likely. In the positive ion mode, a unique acetonitrile complex of NaBPh_4 was observed.

Keywords: alkali metal; ammonium ion; cation– π interaction; mass spectrometry; tetraphenylborate

1. Introduction

The alkali metal–arene (1) and ammonium–arene (2) cation– π interactions were explored by mass spectrometry in the early 1980s. During the 1990s, cation– π interactions were postulated by Kumpf and Dougherty (3) as a mechanism to account for the selectivity of potassium-conducting protein channels. The first solid-state channel structure (4) and other evidence (5) showed that the selectivity filter involved carbonyl groups rather than arenes, but the suggestion had already stimulated great interest in cation– π contacts as a weak force interaction (6–8).

Kebarle and co-workers showed by mass spectrometric analysis that potassium cations formed a stable complex with benzene and estimated its enthalpic stabilisation at 19 kcal/mol (1). Meot-Ner and Deakyne also used mass spectrometry to demonstrate arene–ammonium ion interactions (2). Burley and Petsko recognised the possibility of ammonium– π interactions by 1986 when a search of the Protein Data Bank (PDB) revealed close contacts in a number of protein structures (9). A similar, but more recent, survey concerned arene–arginine interactions (10). Sodium–arene interactions were studied by Castleman et al., and found to be stronger than the corresponding K^+ –benzene contact (11). Lisy and co-workers (12) explored selectivity in the gas phase between Na^+ and K^+ . Many additional studies have been undertaken in order to define the scope and occurrence of the cation– π interaction, both theoretically and in a biological context (13). Contributions from the laboratories of Dunbar (14), Wouters (15), Waters (16), Hunter

(17) and many others have solidified the concept as a significant, if weak, molecular recognition force (18).

Our own efforts to understand the sodium–arene interaction began unsuccessfully with an X-ray structural examination of *N,N'*-dibenzyl-4,13-diaza-18-crown-6. The systems were designed in the expectation that a ring-bound Na^+ would receive secondary, apical stabilisation from the sidearm arenes. In fact, the sidearms were turned away from the ring-bound cation, which interacted with the compound's iodide counterion (19). Remarkably, the simple expedient of extending the sidearms from benzyl to arylethyl permitted solid-state structures to be obtained for sodium or potassium π -complexes involving phenyl (20), hydroxyphenyl (21) and indolyl (22). Solid-state evidence was also obtained for alkali metal–arene interactions with double (23) and triple bonds (24). Ultimately, a broad range of solid-state examples was obtained (25).

Among the simplest alkali metal–arene interactions possible are those observed in the known solid-state structures of the tetraphenylborate salts. The tetraphenylborate anion is tetrahedral and offers a cation four individual arenes or two v-shaped pockets in which a cation could be accommodated. Electrostatic considerations suggest that the cation should approach the negatively charged boron as closely as possible. To the extent sterically possible, the cation should insinuate itself between two arenes to maximise the cation– π interaction.

Some study of tetraphenylborate salts has been reported. Interactions between the C–H group of imidazole and an arene in BPh_4^- were studied in both solid and solution phases (26). Interactions were also

*Corresponding author. Email: gokelg@umsl.edu

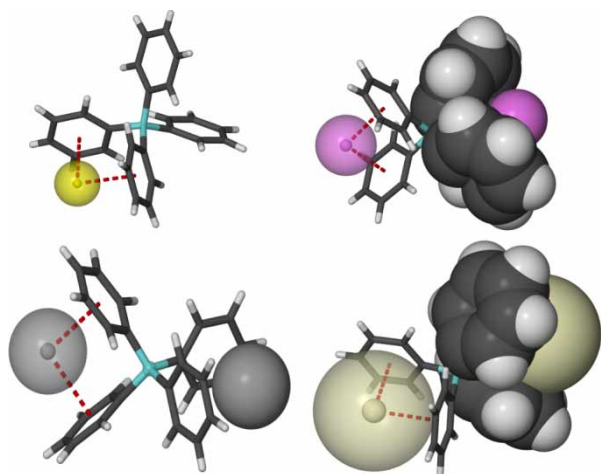


Figure 1. Solid-state structures of NaBPh₄ (1, yellow cation), KBPh₄·K⁺ (2, K⁺, magenta cation), RbBPh₄·Rb⁺ (3, Rb⁺, grey cation) and CsBPh₄·Cs⁺ (4, Cs⁺, cream cation).

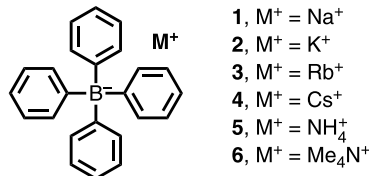
examined between BPh₄⁻ and cations ligated by sigma-donors (27, 28). Ion-selective electrodes have been developed that use the pi-coordinating ability of BPh₄⁻ for function (29). The effort most closely related to our own interest involved a solid-state NMR study of sodium and potassium BPh₄⁻ salts by Wu and co-workers (30). Zhu and co-workers showed by deuterium NMR studies that polycyclic aromatic hydrocarbons interacted more strongly with Cs⁺ cation than with Na⁺, K⁺ or Rb⁺ in aqueous methanol solutions (31).

The study reported here was prompted by two questions. First, do the solid-state structures of MBPh₄ reflect only the packing matrix for these salts? The symmetrical arrangement of the anions, which surround each cation with four arenes, is obviously efficient but does not indicate whether the stronger Lewis acid (i.e. Na⁺) would be favoured over a larger cation such as Cs⁺. Second, the finding of Zhu and co-workers that

aromatic hydrocarbons favoured Cs⁺ over the other ions seemed surprising. Direct gas-phase competition experiments should provide evidence one way or the other. The results of a mass spectrometric study involving both positive and negative ionisation methods are reported here.

2. Results and discussion

Compounds 1–4 are Na⁺, K⁺, Rb⁺ and Cs⁺, tetraphenylborate salts, respectively. Compound 5, NH₄⁺BPh₄⁻, is not an alkali metal salt, but it is of obvious interest in this context. Lithium tetraphenylborate is not included in these studies in part because it has a significant covalent behaviour (32). The only structure available in the Cambridge Structural Database (CSD) is for the hydrated salt (CSD: YIRRIA) (33). X-ray structures are available for 1–5 in the CSD. The solid-state structure of tetramethylammonium tetraphenylborate (6) is also reported (34) and comparisons with it are made below.



2.1 Solid-state structures of tetraphenylborate salts

The solid-state structures for NaBPh₄ (1, CSD: ZZZUPI01), KBPh₄ (2, CSD: KTPHEB02), RbBPh₄ (3, CSD: RBPBOR), CsBPh₄ (4, CSD: ZZZURS01), NH₄BPh₄ (5, CSD: AMPHEB02) and NMe₄BPh₄ (6, CSD: MATPHB) have been reported. Structures generated from the coordinates ((35); www.Pov-Ray.org) are shown in Figure 1. The details of the angles and distances are summarised in Table 1.

Table 1. Summary of tetraphenylborate crystal structure data.

Salt	Descriptor ^a	Data in Å			Data in degrees	
		B ↔ M ⁺ dist. Å ^b	Calc'd B ↔ M ⁺ ^c	M ⁺ –centroid ^d	C ¹ –B–C ¹ angle ^e	Centroid–B–centroid ^f
NaBPh ₄	ZZZUPI10	4.002	3.470	3.028	103.68, 103.68	97.00, 97.00
KBPh ₄	KTPHEB02	3.904	3.906	2.960	103.41, 103.41	96.87, 96.87
RbBPh ₄	RBPBOR	4.026	4.125	3.041	103.76, 103.82	96.90, 96.92
CsBPh ₄	ZZZURS01	4.168	4.379	3.158	104.06, 104.06	97.76, 97.78
NH ₄ BPh ₄	AMPHEB02	4.002	–	3.027	103.65, 103.65	97.00, 97.00
Me ₄ NBPh ₄	MATPHB	5.580	–	4.402	102.04, 104.90	95.73, 103.63

^a Cambridge Structural Database.

^b Distance from a cation or N to boron measured with Mercury software.

^c Calculated using Gaussian 03W, see Section 4.

^d Distance from a cation or N to either centroid.

^e Angle between C¹ of each benzene and boron.

^f Angle between each centroid and boron.

All of the cations [Na^+ , K^+ , Rb^+ , Cs^+ , NH_4^+ and $\text{N}(\text{CH}_3)_4^+$ [note that NH_4^+ and $\text{N}(\text{CH}_3)_4^+$ are not shown in Figure 1]] are situated approximately symmetrically among the four arenes of two adjacent $\text{Ph}-\text{B}^--\text{Ph}$ clefts. This arrangement places each cation proximate to four electron-rich benzene rings and as close as possible to the negative charges on boron.

The ionic radii of Na^+ , K^+ , Rb^+ and Cs^+ increase monotonically, but the B^--M^+ distances, obtained from the solid-state structures, show that the $\text{M} \leftrightarrow \text{B}$ distance in NaBPh_4 is longer than in KBPh_4 and nearly as long as in the Rb complex. This seemed surprising considering that the counteranions are identical and Na^+ is the smallest of the three cations. The data are recorded in Table 1.

Table 1 also shows data for bond angles and various distances. Each BPh_4^- ion has four angles: those shown are for the arenes on the sides facing the cation. These angles are all smaller than the expected tetrahedral angle of 109.5° . The external angles are, as expected, correspondingly larger and are not discussed here. It is interesting to note that the arenes bend towards the cations, presumably to shorten the cation– π contact distance. The average deformation of the angle between the arenes for the metallic tetraphenylborates is $13.2 \pm 0.6^\circ$.

The boron–cation distance is consistent throughout the solid-state matrix, measured along any axis. Figure 2 compares the observed and calculated (Gaussian 03W) M^+-B^- distances. The observed distances were obtained from the X-ray structural data identified above. When each trend was modelled as linear, the calculated line gave $r^2 = 0.99$ but the attempted linear fit for the observed distances was an obviously unacceptable ($r^2 =$) 0.29.

Ion size and the charge-to-size ratio are not thought to control cation– π interactions. Kumpf and Dougherty (3) predicted the order $\text{K}^+ > \text{Rb}^+ \gg \text{Na}^+$ for binding between benzene and these cations in aqueous solution based on an electrostatic model. Caldwell and Kollman showed that polarisability was an important additional consideration for molecular mechanical computations of cation– π interactions (36). Zhu et al. (31), in their

aqueous methanol studies with benzene and polycyclic aromatic hydrocarbons, reported an order of decreasing complexation strength of $\text{Cs}^+ > \text{K}^+ > \text{Rb}^+ > \text{Na}^+$. The order for the latter three cations correlates well with that calculated using a simple electrostatic model. The Gaussian software reports Mulliken charges, which confirm the order reported (37). The experimental result suggesting that Cs^+ interacts especially strongly with arenes seems counter-intuitive but can be examined for the gas phase using mass spectrometry as described below.

2.2 Mass spectrometric assay

Mass spectrometry was used early (1, 2) and has been applied frequently in the study of cation– π interactions (see above). Aggregates can be detected in both negative and positive ion modes. The salts themselves, MBPh_4 , are neutral and not observed. It is assumed that these are present, if not predominant, in all experiments. In the positive ion mode, we expect to observe $[(\text{M}^+)_2 \times (\text{BPh}_4^-)]$ which has a positive charge. Higher aggregates $[\text{M}_n(\text{BPh}_4)_{n-1}]^+$ would also be observed as a negatively charged species. In the negative ion mode, $[\text{M}^+(\text{BPh}_4^-)_2]$ would be observed as would such higher aggregates as $[\text{M}_n(\text{BPh}_4)_{n+1}]^-$. The spectra show relative abundance on the ordinate axis, which is the observed ion current normalised to the most abundant (parent) peak set to 100%.

2.2.1 Negative ion mass spectrometry

Mass spectrometric analyses were conducted using a JEOL MStation (JMS-700) mass spectrometer equipped with an electrospray ionisation source, operating in the negative ion mode and scanning from m/z 100 to 1600. Negative ion experiments for individual salts were run at a concentration of $2 \times 10^{-4} \text{ M}$ in CH_3CN solution. Only three peaks were observed in the mass spectrum for NaBPh_4 . They were m/z 319 (100%), 661 (60%) and 1003 (~1%). These peaks correspond to BPh_4^- , $[\text{Na}(\text{BPh}_4)_2]^-$ and $[\text{Na}_2(\text{BPh}_4)_3]^-$, respectively. As noted above, the neutral salt NaBPh_4 cannot be observed by an ion detector. The relative intensities of the cluster peaks (e.g. $[\text{Na}_2(\text{BPh}_4)_3]^-$) were, as expected, greater at higher salt concentrations (data not shown). The mass spectrum is shown in Figure 3.

Similar, but not identical, data were obtained for KBPh_4 , RbBPh_4 , CsBPh_4 , NH_4BPh_4 and NMe_4BPh_4 . In all cases, the BPh_4^- ion (m/z 319) is the base peak but clusters involving a cation and two anions $[\text{MX}_2]^-$ as well as two cations and three anions $[\text{M}_2\text{X}_3]^-$ are also typically observed. The latter peak is weak in all cases but nearly undetectable in the NaBPh_4 and Me_4NBPh_4 cases. The $[\text{M}(\text{BPh}_4)_2]^-$ ion has a relative abundance of $58 \pm 3\%$ for sodium, potassium

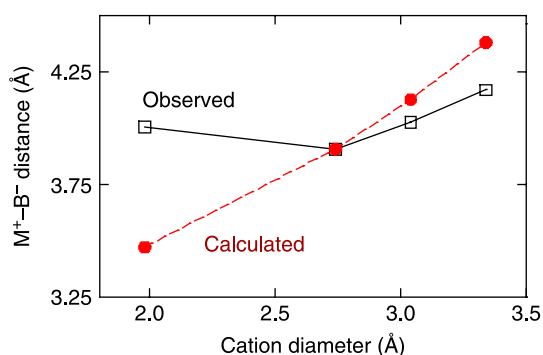


Figure 2. Calculated and observed $\text{M}^+ \cdots \text{B}^-$ bond distances for (left to right) NaBPh_4 , KBPh_4 , RbBPh_4 and CsBPh_4 .

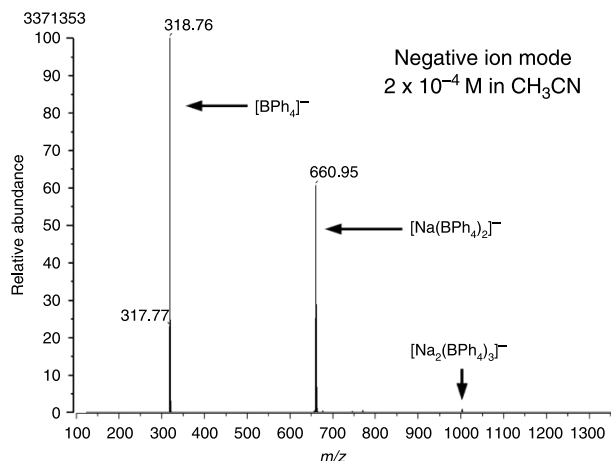


Figure 3. Negative ion ESI spectrum of NaBPh₄, 2×10^{-4} M in CH₃CN.

and ammonium cations ($\text{BPh}_4^- = 100\%$). The abundance of $[\text{M}(\text{BPh}_4)_2]^-$ ion is significantly higher (96%) for $\text{M} = \text{Cs}^+$ and significantly lower (30%) for $\text{M} = \text{NMe}_4^+$. The data, summarised in Table 2, showed good consistency over three separate experiments. The values reported for the abundances of $[\text{M}(\text{BPh}_4)_2]^-$ were in the range of ± 3 to $\pm 5\%$.

Based simply on the Lewis acidity of the metal cations, one would predict the trend: $\text{Na}^+ > \text{K}^+ > \text{Rb}^+ > \text{Cs}^+$. The sizes of the cations increase in the order $\text{Na}^+ < \text{K}^+ \sim \text{NH}_4^+ < \text{Rb}^+ < \text{Cs}^+ < \text{Me}_4\text{N}^+$. As noted above, computational results (3) suggested that the aqueous-phase binding strengths for $[\text{M}\cdot\text{C}_6\text{H}_6]^+$ diminished in the order $\text{K}^+ > \text{Rb}^+ \gg \text{Na}^+$. Caesium was not included in the study. In our (gas phase) study, the $\text{M}(\text{BPh}_4)_2^-$ ion abundance increased in the order $\text{NMe}_4^+ < \text{Na}^+ \sim \text{K}^+ \sim \text{NH}_4^+ < \text{Rb}^+ < \text{Cs}^+$. The order we observe for complexation of BPh_4^- is $\text{Na}^+ \sim \text{K}^+ < \text{Rb}^+$, which is obviously different from the benzene prediction: $\text{K}^+ > \text{Rb}^+ \gg \text{Na}^+$. Still, benzene is a nearly two-dimensional, uncharged molecule and BPh_4^- has four rings and is an anion. It is interesting to note, however, that

the abundance for caesium was nearly twice that for sodium, potassium or ammonium and three times that of tetramethylammonium. We interpret this to mean that caesium does, indeed, have an unusually high affinity for arenes, as asserted by Zhu et al., based on NMR experiments (31). This seems not to be simply a size-based phenomenon as tetramethylammonium cation is larger still, singly charged and less capable of organising two tetraphenylborate anions.

2.2.2 Positive ion mass spectrometry

The experiments were conducted as noted above but the instrument was operated in the positive ion mode while scanning from m/z 100 to 1600. These experiments were run at a salt concentration of 2×10^{-4} M in CH₃CN solution. The number of peaks observed in the positive mode was similar to the number apparent in the negative ion experiments, but the spectra were much noisier. We attribute this to residual hydrophilic cationic species not fully purged from the system. As in the negative mode, cluster ions are apparent. In the case of **1–4**, spraying M^+BPh_4^- in CH₃CN typically resulted in two dominant peaks. These correspond to $(\text{M}^+)_2\text{BPh}_4^-$ and $(\text{M}^+)_3(\text{BPh}_4^-)_2$.

The positive ion spectrum of NaBPh₄ is shown in Figure 4. The base peak is $(\text{Na}_2\text{BPh}_4)^+$ and a small peak (relative abundance $\sim 15\%$) corresponds to $[\text{Na}_3(\text{BPh}_4)_2]^+$. The positive ion spectrum of NaBPh₄ was unique in this study because a major (abundance = 75%) peak was apparent at m/z 406 that corresponds to $[(\text{Na})_2\text{BPh}_4\cdot\text{CH}_3\text{CN}]^+$. Typically, the solvent is stripped in the electrospray ionisation process. No other peak that includes the solvent was observed in any other spectrum of **1–5**, when conducted either in the positive or negative ion mode. The identity of the m/z 406 peak was confirmed by an analysis of its isotope distribution (data not shown). Sodium cation has the highest Lewis acidity of any cation in this series and it is expected to have the highest electrostatic affinity for acetonitrile.

Table 2. Negative ion ESI-MS analysis of tetraphenylborate salts^a.

Compound	Observed peaks and relative abundances ^b				
	BPh_4^- (m/z 319) (%)	$[\text{M}(\text{BPh}_4)_2]^-$ (%)	m/z	$[\text{M}_2(\text{BPh}_4)_3]^-$ (%)	m/z
1 NaBPh ₄	100	58	661	~ 1	1003
2 KBPh ₄	100	58	677	8	1035
3 RbBPh ₄	100	80	723	5	1126
4 CsBPh ₄	100	96	771	4	1222
5 NH ₄ BPh ₄	100	59	656	4	992
6 NMe ₄ BPh ₄	100	30	712	–	–

^a See text for experimental information.

^b Peak abundance (isotope effect included) was recorded and compared with the parent peak, which is set to 100%. Each abundance value represents three individual experiments with a variation of less than or equal to $\pm 5\%$.

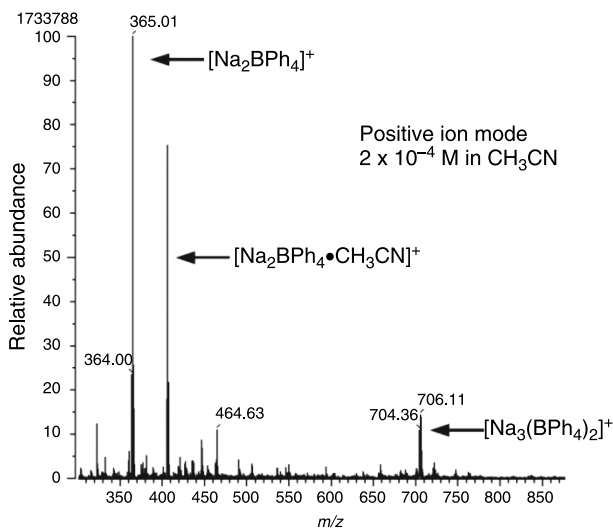


Figure 4. Positive ion ESI-MS of NaBPh₄ (**1**) sprayed in CH₃CN solution.

By far, the most complex spectrum was observed for NH₄BPh₄, **5**, for which numerous mixed cation peaks involving Na⁺ were apparent (spectrum not shown). In contrast to the other positive ion spectra, the spectrum obtained for CsBPh₄ (**4**) was remarkably free of competing Na⁺ ions, which is shown in Figure 5.

The data acquired for the series of compounds **1–6** are summarised in Table 3. For all of the salts that were analysed except KBPh₄, the [M₃(BPh₄)₂]⁺ ion was the base peak. For KBPh₄, the (M₂BPh₄)⁺ and [M₃(BPh₄)₂]⁺ peaks fall within the range of 97 ± 3% but the intensity of the [K₃(BPh₄)₂]⁺ peak is surprising as K⁺ is not the strongest Lewis acid in this family.

It is notable that the base peak in the positive ion mode for K⁺ is a cluster having the elements [K₃(BPh₄)₂]⁺.

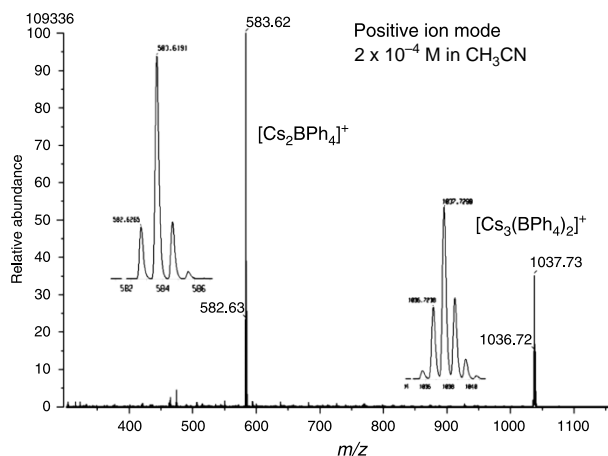


Figure 5. Positive ion ESI-MS of CsBPh₄ (**4**) sprayed in CH₃CN solution. The insets show the isomer distributions of the adjacent peaks.

The base peaks for NaBPh₄, RbBPh₄, CsBPh₄ and NH₄BPh₄ all correspond to the general ion M₂BPh₄⁺. Potassium cation is neither the most nor the least charge-dense, nor is it the largest or the smallest in the group. It is interesting to note that when the anion was changed from tetraphenylborate to *tetrakis*(*p*-chlorophenyl)borate, the [M₃X₂]⁺ ion still dominated (data not shown).

We were surprised by the extent to which residual Na⁺ ions incorporated into clusters when other salts were sprayed. The near absence of Na⁺ in the CsBPh₄ spectrum was noted above. By contrast, when NH₄BPh₄ (**5**) was sprayed in CH₃CN, a peak corresponding to [NaNH₄BPh₄]⁺ was nearly as abundant as the [(NH₄)₂BPh₄]⁺ peak. When the NH₄⁺ cation was replaced by (CH₃)₄N⁺, the sodium-containing peak was hardly detectable when Me₄NBPh₄ was sprayed in acetonitrile.

2.3 Competition experiments

It was of obvious interest to compare a sigma-donor anion (Cl⁻) with BPh₄⁻. Two solutions were prepared (each 100 μM in CH₃CN) for study: 1:1 NaCl + KBPh₄ and 1:1 NaBPh₄ + KCl. Each mixture was sprayed and analysed in the negative ion mode with comparable results. Three peaks were observed at relative abundances > 5%. They were BPh₄⁻ (*m/z* 319, base), [Na(BPh₄)₂]⁻ and [K(BPh₄)₂]⁻. No significant ion that included Cl⁻ was observed. A similarly prepared mixture of KCl and RbBPh₄ showed (negative mode) three significant peaks. They were BPh₄⁻ (base peak), [K(BPh₄)₂]⁻ (*m/z* 677) and [Rb(BPh₄)₂]⁻ (*m/z* 723). Three peaks were also observed when KCl and CsBPh₄ were mixed. The base peak was BPh₄⁻, the second most abundant peak was [Cs(BPh₄)₂]⁻ (*m/z* 771) and a minor peak was observed for [K(BPh₄)₂]⁻. In these comparisons involving different cations versus K⁺ and the potential for Cl⁻ or BPh₄⁻ association, Cs⁺ and BPh₄⁻ appear to be dominant.

In the positive ion mode, a similar experiment gave more complicated spectra. In this case, KCl and CsBPh₄ solutions were prepared (500 μM, 1:1 CH₃CN:CH₃OH) and then sprayed. Six peaks were detected in the positive ion mode. Only four of these had abundances > 5%. They were [KCsBPh₄]⁺ (*m/z* 490, 11%), [Cs₂BPh₄]⁺ (*m/z* 584, base), [KCs₂(BPh₄)₂]⁺ (*m/z* 944, 6%) and [Cs₃(BPh₄)₂]⁺ (*m/z* 1038, 25%). Peaks attributable to the composition [K₂BPh₄]⁺ and [K₂Cs(BPh₄)₂]⁺ were also observed, but their abundances were only about 1%. Again, the most significant ions were attributable to Cs⁺ and BPh₄⁻ complexes. The K⁺ complex was less significant and Cl⁻ complex was not detected.

In order to directly compare cations, we mixed equimolar solutions of NaBPh₄ and MBPh₄ (together 200 μM salts) in CH₃CN and analysed the solution using the negative ion mode of electrospray (three runs). We compared the abundance of the [M(BPh₄)₂]⁻ peak

Table 3. Positive ion electrospray mass spectrometry of tetraphenylborate salts.

Compound	Relative abundance			
	$(M_2BPh_4)^+$ (%)	$[M_3(BPh_4)_2]^+$ (%)	$[(Na\cdot M)BPh_4]^+$ (%)	$[M_4(BPh_4)_3]^+$ (%)
1 NaBPh ₄	100	14	–	<5
2 KBPh ₄	94	100	23	<5
3 RbBPh ₄	100	73	21	<5
4 CsBPh ₄	100	35	<5	<5
5 NH ₄ BPh ₄	100	14	92	<5
6 NMe ₄ BPh ₄	100	<3	<3	–

observed for the second cation with the $[Na(BPh_4)_2]^-$ peak, arbitrarily normalised to 1.0. Compared with the value for Na⁺ of 1.0, the following abundances were observed: K⁺, 1.2; Rb⁺, 2.5; and Cs⁺, 5.0. In direct competition, the order is Na⁺ ~ K⁺ < Rb⁺ < Cs⁺.

The data shown in Table 2 compare the abundances of $[Na(BPh_4)_2]^-$ and $[M(BPh_4)_2]^-$ for the salts 1–4. If we set the abundance of the $[Na(BPh_4)_2]^-$ to 1.0, the Na:K:Rb:Cs ratio is 1:1:1.4:1.7. In the direct comparison with NaBPh₄, the $[M(BPh_4)_2]^-$ ions show an almost identical trend. This further confirms the greater ability of Cs⁺ to interact with BPh₄[–]. The crystal structures illustrated in Figure 1 show that Rb⁺ is large enough that no steric effect is likely to play a role. This confirms the high affinity of Cs⁺ for BPh₄[–] and, by extension, for arenes generally.

A further experiment was undertaken in which a solution (200 μM, CH₃CN) containing equimolar Na⁺, K⁺, Rb⁺ and Cs⁺ BPh₄[–] salts was sprayed and analysed in the positive mode. Such an experiment carries with it the inherent error of observing residual cations in addition to those present in the solution (see above). Seven ions were detected in which a single BPh₄[–] ion appeared to accompany two cations. The masses of five ions could be fitted to the formula $[M_3(BPh_4)_2]^+$. The data are summarised in Table 4. Nine of the 12 significant ions include the caesium cation. The four ions having the highest relative abundances all contain one or more caesium ions.

Table 4. Four-cation competition study^a.

$[M_1M_2BPh_4]^{+b}$			$[M_1M_2M_3(BPh_4)_2]^{+b}$		
<i>m/z</i>	Amt. ^c	M ₁ M ₂	<i>m/z</i>	Amt. ^c	M ₁ M ₂ M ₃
365	23	Na ₂	849	10	K ₂ Cs
381	17	NaK	896	14	KRbCs
427	15	NaRb	944	17	KCs ₂
474	45	NaCs	989	17	RbCs ₂
490	30	KCs	1037	9	Cs ₃
537	33	RbCs			
584	54	Cs ₂			

^a Equimolar NaBPh₄, KBPh₄, RbBPh₄ and CsBPh₄, in CH₃CN, ESI-MS positive ion mode.

^b Observed ion.

^c Relative abundance.

2.4 The gas-phase cation–pi interaction

The cation–pi interaction is a weak force. The tetraphenylborate anion possesses four electron-rich benzene rings that are positioned so that two within the same structure may simultaneously interact with a cation. The charge on boron is both highly diffuse and sterically hindered. It is not expected to directly interact with a complexed (associated) cation. The solid-state structures of NaBPh₄, KBPh₄, RbBPh₄ and CsBPh₄ all suggest that orderly and largely symmetrical interactions should occur between the cation and the anion. The calculated M–B distances for the MBPh₄ salt (complex) in the gas phase increase monotonically from sodium through caesium. The observed bond distances in the solid state do not agree: sodium cation has a longer than expected distance. This is likely due to the steric demand of the large anion. The K–B, Rb–B and Cs–B distances fall on a straight line, whether the distances are calculated or observed. There is no indication that caesium will behave differently with tetraphenylborate than do the other cations. In fact, caesium shows a higher affinity for tetraphenylborate than do the other cations, in a variety of negative and positive ion electrospray experiments.

Zhu et al. (31) have reported deuterium NMR experiments with both deuterated benzene and polyaromatic hydrocarbons that suggest a special affinity of Cs for arenes. They attribute this affinity, which is apparent in the results presented here, to the high polarisability of this cation. Caldwell and Kollman (36) have concluded that polarisability is important in modelling the cation–pi interaction and that generalisation comports with the results presented here.

3. Conclusions

Computations by Kumpf and Dougherty (3) predicted the following binding order with benzene (aqueous phase): K⁺ > Rb⁺ ≫ Na⁺. Zhu et al. (31) found the order Cs⁺ > K⁺ > Rb⁺ > Na⁺ for aqueous methanol using deuterium NMR methods. The order for the latter three cations agrees generally with the aqueous-phase calculations. The order that we observe for the tetraphenylborate anions is Cs⁺ > Rb⁺ > K⁺ ~ Na⁺. Admittedly, this binding order

reflects contacts with electron-rich arenes, which are expected to be more polarisable than benzene. We agree with the Zhu et al. finding that Cs^+ shows the strongest arene–cation interaction but conclude that the polarisability dominates over electrostatics for an electron-rich arene and a weakly Lewis acidic cation, leading to an apparently reasonable order. The Mulliken charge calculation showed that the atomic charge on the metals decreased in the order $\text{Cs}^+ > \text{K}^+ > \text{Rb}^+ > \text{Na}^+$. We note that the validity of this methodology is further supported by two experimental observations. First, ESI-MS shows that only Na^+ includes acetonitrile in a complex cation. Second, only Cs^+ shows ESI-MS spectra that are devoid of interference by other residual cations. The latter observation confirms the order listed above and the former comports with the high Lewis acidity of the Na^+ cation, showing that it is behaving normally in these experiments.

4. Experimental section

4.1 General

NMR spectra were recorded by a Varian Unity Plus 300 MHz NMR spectrometer and a Bruker Avance 300 MHz NMR spectrometer. ^1H NMR was recorded at 300 MHz in CD_3CN solvents and is reported in ppm (δ) downfield from internal TMS unless otherwise noted. ^{13}C NMR was recorded at 75 MHz in CD_3CN unless otherwise stated. ^{11}B NMR was recorded at 96 MHz in CD_3CN unless otherwise stated. Melting points were determined on a Thomas Hoover apparatus in open capillaries and are uncorrected. Sodium, potassium, rubidium, caesium and ammonium tetraphenylborate are the best (non-LC) grade commercially available and were distilled, recrystallised or used without further purification, as appropriate. ESI-MS is the abbreviation for electrospray ionisation mass spectrometry. Acetonitrile is of HPLC grade, which is suitable for mass spectrometry analysis. Fast atom bombardment (FAB) mass spectrum was obtained using a JEOL MStation (JMS-700) mass spectrometer (in UMSL).

4.2 Tetramethylammonium tetraphenylborate ($\text{Me}_4\text{N}\cdot\text{BPh}_4$)

It was prepared by a simplified procedure. Tetramethylammonium chloride (10.96 mg, 10 ml, 0.01 M solution in CH_3CN) and sodium tetraphenylborate (34.22 mg, 10 ml, 0.01 M solution in CH_3CN) were mixed and stirred at room temperature for 1 h. The solvent was evaporated and the residue was crystallised in $\text{CH}_3\text{CN}-\text{H}_2\text{O}$ (1:9, v/v). A white solid, 25.01 mg (64%), was obtained. Melting point: 368–370°C. ^1H NMR (CD_3CN , 300 MHz) δ (ppm): 3.04 (s, 12H), 6.84 (t, 4H, $J = 7.20$ Hz), 7.00 (t, 8H, $J = 7.35$ Hz), 7.27 (m, 8H). ^{11}B NMR (CD_3CN , 96 MHz) δ (ppm): 66.62 (s). ^{13}C NMR (CD_3CN , 75 MHz) δ (ppm):

56.66 (CH_3), 123.16 (C-4), 126.96 (C-2, C-6), 137.15 (C-3, C-5), 163.40 (C-1). MS-FAB (negative): m/z ($\text{Me}_4\text{N}\cdot\text{BPh}_4 + \text{BPh}_4$, $\text{C}_{52}\text{H}_{52}\text{NB}_2$) calculated 712.4286, found 712.4302.

4.3 Electrospray ionisation mass spectrometry

Mass spectra were obtained using a JEOL MStation (JMS-700) mass spectrometer equipped with an electrospray ionisation source, operating in the negative or positive ion mode and scanning from m/z 100 to 1600. Slits were set to achieve a resolution of about 2000. Stock solutions were prepared in CH_3CN at 1 mM for each tetraphenylborate salt and in CH_3OH at 1 mM for NaCl and KCl. The tested mixing solution was injected and kept at a flow rate of 50 $\mu\text{l}/\text{min}$ using a Harvard syringe pump. The spray voltage was 2.00 kV, and the capillary temperature (desolvating temperature) was 200°C. Each trial was processed using the MSMP9020D software supplied by JEOL with a minimum of 21 scans averaged for the final spectral presentation. Mass values in Figures 4 and 5 were not corrected. They varied from theory by 1 mass unit.

4.4 Computational details

All calculations were performed using the Gaussian 03W suite of programs. The B3LYP as one of the density functional theory methods was used for all geometry optimisation and single-point energy calculations. The method combines Becke's three-parameter functional (38) with the non-local correlation provided by the correlation functional of Lee et al. (39), which has been shown to be suitable for vibrational frequency calculations and geometry optimisation. We performed the restricted B3LYP with the LanL2DZ (D95V on first row, Los Alamos ECP plus DZ on Na–Bi; <http://www.gaussian.com>) basis set. For each molecule, several reasonable conformations were calculated to compare the final energies of stable conformations and the one having the lowest energy was chosen as the final structure. For the chosen structure, all geometries were completely optimised in the gas phase.

Acknowledgements

We thank the NSF (CHE-0415586) and NIH (GM 36262) for grants that supported this work.

References

- (1) Sunner, J.; Nishizawa, K.; Kebarle, P. *J. Phys. Chem.* **1981**, *85*, 1814–1820.
- (2) Meot-Ner, M.; Deakyne, C.A. *J. Am. Chem. Soc.* **1985**, *107*, 474–479.
- (3) Kumpf, R.A.; Dougherty, D.A. *Science* **1993**, *261*, 1708–1710.

- (4) Doyle, D.A.; Cabral, J.M.; Pfuetzner, R.A.; Kuo, A.; Gulbis, J.M.; Cohen, S.L.; Chait, B.T.; MacKinnon, R. *Science* **1998**, *280*, 69–77.
- (5) Heginbotham, L.; Lu, Z.; Abramson, T.; MacKinnon, R. *Biophys. J.* **1994**, *66*, 1061–1067.
- (6) Dougherty, D. *Science* **1996**, *271*, 163–168.
- (7) Ma, J.C.; Dougherty, D.A. *Chem. Rev.* **1997**, *97*, 1303–1324.
- (8) Gallivan, J.P.; Dougherty, D.A. *Proc. Natl Acad. Sci. USA* **1999**, *96*, 9459–9464.
- (9) Burley, S.K.; Petsko, G.A. *FEBS Lett.* **1986**, *203*, 139–143.
- (10) Flocco, M.M.; Mowbray, S.L. *J. Mol. Biol.* **1994**, *235*, 709–717.
- (11) Guo, B.C.; Purnell, J.W.; Castleman, A.W., Jr. *Chem. Phys. Lett.* **1990**, *168*, 155–160.
- (12) (a) Cabarcos, O.M.; Weinheimer, C.J.; Lisy, J.M. *J. Chem. Phys.* **1998**, *108*, 5151–5154. (b) Cabarcos, O.M.; Weinheimer, C.J.; Lisy, J.M. *J. Chem. Phys.* **1999**, *110*, 8429–8435.
- (13) Scrutton, N.S.; Raine, A.R. *J. Biochem.* **1996**, *319* (Pt 1), 1–8.
- (14) Dunbar, R.C. *J. Phys. Chem. A* **1998**, *102*, 8946–8952.
- (15) (a) Wouters, J. *Protein Sci.* **1998**, *7*, 2472–2475. (b) Dunbar, R.C. *J. Phys. Chem. A* **2000**, *104*, 8067–8074.
- (16) Tsou, L.K.; Tatko, C.D.; Waters, M.L. *J. Am. Chem. Soc.* **2002**, *124*, 14917–14921.
- (17) Hunter, C.A.; Low, C.M.R.; Rotger, C.; Vinter, J.G.; Zonta, C. *Proc. Natl Acad. Sci. USA* **2002**, *99*, 4873–4876.
- (18) Hunter, C.A. *Angew. Chem. Int. Ed. Engl.* **2004**, *43*, 5310–5324.
- (19) (a) Gandour, R.D.; Fronczek, F.R.; Gatto, V.J.; Minganti, C.; Schultz, R.A.; White, B.D.; Arnold, K.A.; Mazzocchi, D.; Miller, S.R.; Gokel, G.W. *J. Am. Chem. Soc.* **1986**, *108*, 4078–4088. (b) Arnold, K.A.; Viscariello, A.M.; Kim, M.; Gandour, R.D.; Fronczek, F.R.; Gokel, G.W. *Tetrahedron Lett.* **1988**, *29*, 3025–3028.
- (20) De Wall, S.L.; Meadows, E.S.; Barbour, L.J.; Gokel, G.W. *Proc. Natl Acad. Sci. USA* **2000**, *97*, 6271–6276.
- (21) De Wall, S.L.; Barbour, L.J.; Gokel, G.W. *J. Am. Chem. Soc.* **1999**, *121*, 8405–8406.
- (22) De Wall, S.L.; Meadows, E.S.; Barbour, L.J.; Gokel, G.W. *J. Am. Chem. Soc.* **1999**, *121*, 5613–5614.
- (23) Hu, J.; Barbour, L.J.; Gokel, G.W. *Chem. Comm.* **2001**, 1858–1859.
- (24) Hu, J.; Barbour, L.J.; Gokel, G.W. *J. Am. Chem. Soc.* **2001**, *123*, 9486–9487.
- (25) (a) Gokel, G.W.; Barbour, L.J.; Ferdani, R.; Hu, J. *Acc. Chem. Res.* **2002**, *35*, 878–886. (b) Gokel, G.W. *Chem. Commun.* **2003**, *23*, 2847–2852.
- (26) Dupont, J.; Suarez, P.A.; De Souza, R.F.; Burrow, R.A.; Kintzinger, J.P. *Chem. Eur. J.* **2000**, *6*, 2377–2381.
- (27) Fooladi, E.; Dalhus, B.; Rømming, C.; Tilset, M. *Acta Cryst.* **2002**, *C58*, m567–m569.
- (28) Fukin, G.K.; Lindeman, S.V.; Kochi, J.K. *J. Am. Chem. Soc.* **2002**, *124*, 8329–8336.
- (29) Bobacka, J.; Alaviuhkola, T.; Hietapelto, V.; Koskinen, H.; Lewenstam, A.; Lamsa, M.; Pursiainen, J.; Ivaska, A. *Talanta* **2002**, *58*, 341–349.
- (30) Wong, A.; Whitehead, R.D.; Gan, Z.; Wu, G. *J. Phys. Chem. A* **2004**, *108*, 10551–10559.
- (31) Zhu, D.; Herbert, B.E.; Schlautman, M.A.; Carraway, E.R. *J. Environ. Qual.* **2004**, *33*, 276–284.
- (32) Povey, A.F.; Sherwood, P.M.A. *J. Chem. Soc., Faraday Trans. 2* **1974**, *70*, 1240–1246.
- (33) Bakshi, P.K.; Sereda, S.V.; Knop, O. *Can. J. Chem.* **1994**, *72*, 2144–2152.
- (34) CSD: MATPHB. Hoffmann, K.; Weiss, E. *J. Organomet. Chem.* **1974**, *67*, 221–228.
- (35) Barbour, L.J. X-Seed X-Ray Crystallography Program for Windows. <http://www.x-seed.net/> **2003**.
- (36) Caldwell, J.W.; Kollman, P.A. *J. Am. Chem. Soc.* **1995**, *117*, 4177–4178.
- (37) (a) Tsuzuki, M.; Uchimar, T.; Mikami, M. *J. Phys. Chem. A* **2003**, *107*, 10414–10418. (b) Reddy, A.S.; Sastry, N. *J. Phys. Chem. A* **2005**, *109*, 8893–8903. (c) Tateno, M.; Hagiwara, Y. *J. Phys. Cond. Mat.* **2009**, *21*, 064243.
- (38) Becke, A.D. *J. Chem. Phys.* **1993**, *98*, 5648–5652.
- (39) Lee, C.; Yang, W.; Parr, R.G. *Phys. Rev. B* **1988**, *37*, 785–789.